JOURNAL OF SOLID STATE CHEMISTRY 77, 26–32 (1988)

Crystallographic Properties and Optical Energy Gap Values for $(AgCd_2In)_p(CuIn)_{2y}Mn_{4z}Te_4$ ($p + y + z = 1$) Alloys

MIGUEL QUINTERO, PEDRO GRIMA, EUNICE GUERRERO, RAFAEL TOVAR, GERARDO S. PÉREZ, AND JOHN C. WOOLLEY*

Centro de Estudios de Semiconductores, Laboratorio de Cristales, Departamento de Física, Facultad de Ciencias, Universidad de Los Andes, Mérida, Venezuela

Received January 4, 1988; in revised form May 2, 1988

Polycrystalline samples of $(AgCd_2In)_p(CuIn)_{2y}Mn_{4z}Te_4$ ($p + y + z = 1$) alloys were prepared by a melt and anneal technique. Guinier X-ray powder photographs were used to determine equilibrium conditions and lattice parameter values (a and c). Four single-phase fields, two with the normal zinc blende and chalcopyrite structures and two with the chalcopyrite and zinc blende structures in which the Mn atoms show crystallographic ordering on the cation sublattice are found to exist in the diagram. It was found that the variation of a was practically linear with composition and so could not be used to determine the boundaries between the four fields. Optical absorption measurements were carried out to give values of the optical energy gap E_0 for all single-phase samples. While E_0 varied linearly with composition inside a phase field, the resulting lines had different aiming points at $z = 1.0$, the values being 2.83 eV for the Mn-disordered zinc blende phase, 1.90 eV for the Mn-ordered zinc blende phase, and 1.35 eV for the Mn-ordered chalcopyrite phase. Thus these values of E_0, being characteristic of the structure, give a very good indication of the phase boundaries.

I. Introduction

The names semimagnetic semiconductor alloy or diluted magnetic semiconductor have been applied to materials obtained by substituting a paramagnetic ion on the cation sublattice of a normal compound semiconductor. The presence of the paramagnetic ion causes differences in the semiconductor behavior, particularly in a magnetic field, from that of a normal semiconductor and also introduces interesting magnetic behavior. If the alloy to be produced is to be a semiconductor, then the electron to atom ratio must be conserved, i.e., on the average, the magnetic ions must replace nonmagnetic cations of the same valence.

Most of the work (*1*, *2*) on such alloys has been concerned with the replacement by manganese of the divalent elements Zn, Cd, and Hg, e.g., $Cd_{1-z}Mn_zTe$. However, it is possible to produce similar materials from the chalcopyrite *I–III–VI*$_2$ compounds, the ternary analogs of the *II–VI* compounds. If the paramagnetic ion to be included is divalent Mn, then to retain the electron to atom ratio, it is necessary to replace one *I* and one *III* cation simultaneously by two manganese atoms.

The crystallography and optical energy

* Permanent address: Physics Department, University of Ottawa, Ottawa, Ontario, Canada K1N 6N5.

0022-4596/88 $3.00

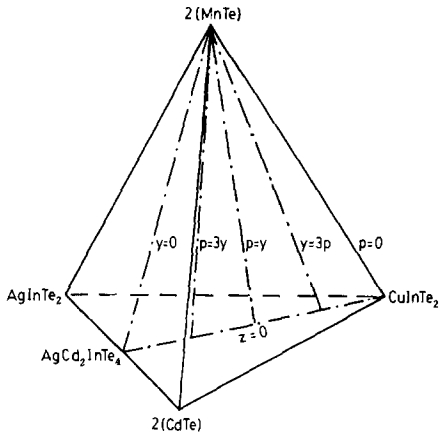

FIG. 1. General diagram showing the section investigated in the present work. Lines investigated with $y = 0$, $p = 3y$, $p = y$, $y = 3p$, and $z = 0$ are shown dash-dotted.

gap values for the alloy system $(CuIn)_{1-z}Mn_{2z}Te_2$ and $(AgIn)_{1-z}Mn_{2z}Te_2$ were published previously (*3, 4*). Aresti *et al.* (*5*) reported the $T(z)$ diagram of the $(CuIn)_{1-z}Mn_{2z}Te_2$ alloys and in more recent work (*6, 7*), the $T(z)$ diagrams of $(CuIn)_{1-z}Mn_{2z}Te_2$, $(AgIn)_{1-z}Mn_{2z}Te_2$, and $(AgGa)_{1-z}Mn_{2z}Te_2$ were investigated. Woolley *et al.* (*8*) studied the relation between the crystallography, optical, and magnetic properties of the $(I\text{–}III)_{1-z}Mn_{2z}Te_2$ (I = Cu, Ag; III = In, Ga) alloy systems. Here, the study of the chalcopyrite alloys has been extended to other sections of the general system $Cd_{2w}(AgIn)_x(CuIn)_yMn_{2z}Te_2$ ($w + x + y + z = 1$).

II. Materials To Be Investigated

The system $Cd_{2w}(AgIn)_x(CuIn)_yMn_{2z}Te_2$ can be conveniently represented by a regular tetrahedron as shown in Fig. 1 with 2(CdTe), $AgInTe_2$, $CuInTe_2$, and 2(MnTe) at the four apices. The systems $Cd_{2w}(CuIn)_yMn_{2z}Te_2$ (*3*), $Cd_{2w}(AgIn)_xMn_{2z}Te_2$ (*4*), and $Cd_{2w}(AgIn)_x(CuIn)_yTe_2$ (*9*) already reported form three faces of the tetrahedron. The other face, $(AgIn)_x(CuIn)_yMn_{2z}Te_2$ is still being studied. In the present work, the section given by $x = w$ ($= p/2$) is being studied. This section has the form $Cd_p(AgIn)_{p/2}(CuIn)_yMn_{2z}Te_2$ which can be more conveniently written as $(AgCd_2In)_p(CuIn)_{2y}Mn_{4z}Te_4$. The section is an isosceles triangle in Fig. 1, but can conveniently be represented by the usual equilateral triangle with coordinates p, y, and z as shown in Fig. 2. To facilitate comparison of results, samples were made at compositions along the lines in the diagram at constant p/y ratios, i.e., $y = 0$, $p = 3y$, $p = y$, $y = 3p$, and $p = 0$, and at various fixed values of z as shown in Figs. 1 and 2.

III. Preparation of Samples and Experimental Measurements

The initial requirement of any investigation of alloy systems of this type is to determine the composition range over which single-phase solid solution occurs and hence this was the first work carried out in the present program. All of the alloys used were produced by the usual melt and anneal

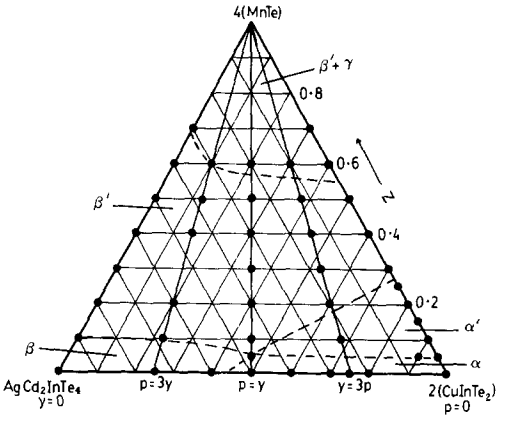

FIG. 2. Isothermal section of the $(AgCd_2In)_p(CuIn)_{2y}Mn_{4z}Te_4$ diagram at 200°C. ●, Compositions investigated; ---, phase boundaries; α, Mn-disordered chalcopyrite; α', Mn-ordered chalcopyrite; β, Mn-disordered zinc blende; β', Mn-ordered zinc blende; γ, NiAs phase of MnTe.

technique (*10*). The components of each 1.5-g sample were sealed under vacuum in small quartz ampoules which had previously been carbonized to prevent interaction of the alloy with the quartz, melted together at 1150°C, and then annealed to equilibrium at 600°C. As in all such multicomponent alloys, the appropriate temperature of anneal is not easily determined until the T vs composition phase diagram is known for each section. However, the results for the sections $(AgIn)_{1-z}Mn_{2z}Te_2$ and $(CuIn)_{1-z}Mn_{2z}Te_2$ (*6*), already investigated, showed that an annealing temperature of 600°C was satisfactory in those cases. Thus this temperature was used in the present work and the final results showed this to be satisfactory. It has been found that at least 20–30 days of annealing is necessary to obtain the equilibrium conditions at 600°C since long-range diffusion may be required after the initial cooling from the melt. However, the transitions from zinc blende to chalcopyrite, which frequently occur below 600°C in these systems, involve only short-range diffusion and so can usually occur in the time required to cool the sample down to room temperature if the sample is left in the furnace which has been switched off. Guinier X-ray powder photographs were used to check the equilibrium conditions of each sample and to determine whether a single-phase form was present. Values of lattice parameters were determined as a function of the composition variables, germanium being used as an internal standard in the Guinier photographs.

Slices of each single-phase sample were cut and thinned down to give specimens for optical absorption work, standard measurements (*11*) being made using a Cary 17 spectrometer. Values of $1/d\ln(I_0/I_t)$, where d is the thickness, I_0 the incident intensity, and I_t the transmitted intensity, were determined as a function of photon energy $h\nu$ and corrected by subtracting a background value to give the absorption coefficient α. It was found that the background absorption in many of these samples was high, so that the slices needed to be ground down to a thickness d of the order of 100 μm or less to obtain any measurable transmitted intensity.

IV. X-Ray Results

It was found that for all of the single-phase samples, the X-ray photographs showed the usual lines typical of the zinc blende structure of CdTe. In each case, a standard cubic analysis was used to give a value of the lattice parameter a and these values are shown plotted as a function of z for constant p/y ratio in Fig. 3, and graphs of a vs y for the lines $z = 0$ and $z = 0.5$ are shown in Fig. 4. Since for values of z between these two limits the curves would lie between the two shown and the separation would be comparable with the experimental scatter, for the sake of clarity these lines have not been included. At high z values, lines of the nickel arsenide structure of MnTe were observed in addition to the ap-

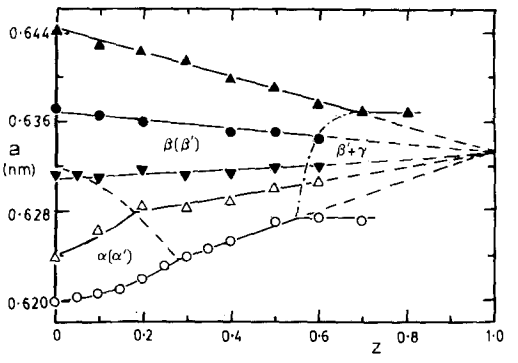

FIG. 3. Variation of lattice parameter a with z for various p/y ratios. The extrapolated value of a is that for a hypothetical MnTe in zinc blende structure. (○) $p = 0$, (△) $y = 3p$, (▼) $p = y$, (●) $p = 3y$, (▲) $y = 0$. ---, Boundary between chalcopyrite and zinc blende fields. ·-·-·, Boundary between single-phase and two-phase fields.

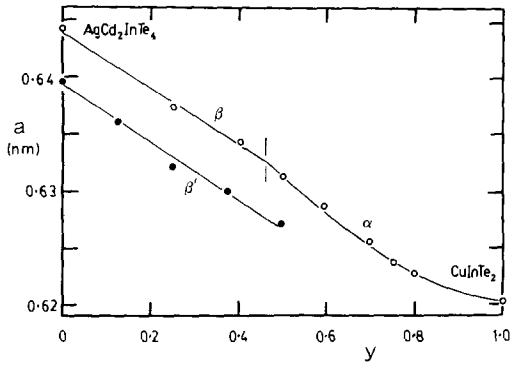

FIG. 4. Variation of lattice parameter a with y for the lines $z = 0$ (○) and $z = 0.5$ (●). α, chalcopyrite; β, zinc blende; β', Mn-ordered zinc blende.

parent zinc blende lines. Values of the zinc blende a parameter were determined for these two-phase samples and these also are shown in Fig. 3. In the case where there is appreciable variation of a with z, the limit of single-phase solid solution can easily be determined as the point of slope discontinuity in the line of a vs z. This method was used to give the limits of solid solution for the lines $p = 0$ and $y = 0$. However for the lines $p = 3y$, $p = y$, and $y = 3p$ the variation of a with z was too small to allow this method to be used. Thus the limits of solid solution in the zinc blende structure were determined by the observation of MnTe lines indicating two-phase behavior. The limits shown in Fig. 2 were estimated in this way. The lines of a vs z in the single-phase region appeared to be linear within the limits of experimental except for the cases $p = 0$ and $y = 3p$ at low z values, i.e., close to $CuInTe_2$, where there is appreciable curvature.

It is well known (*12*) that $CuInTe_2$ is tetragonal with $c/a = 2$ and so gives the pseudocubic results indicated above. For alloys with high values of y, the normal chalcopyrite ordering lines were observed with relatively low intensity, and this intensity decreased as the composition was moved away from $y = 1$. Such a reduction is to be expected since as y is decreased in any direction, the difference in the scattering power of the two cation sublattices is reduced and this difference is the quantity which determines the intensity of the ordering lines. In addition, it is possible that the degree of chalcopyrite ordering is reduced at the same time. This reduction in intensity of the ordering lines has been used to indicate the boundary of the chalcopyrite field, but a second criterion probably gives a more accurate estimate of this boundary.

This second indication of the range of chalcopyrite structure is given by the variation of a with composition on the lines $p = 0$, $y = 3p$, and $z = 0$ since, as indicated above, changes in slope occur in the graphs of a vs composition. As is seen from Figs. 3 and 4, the variation of a with composition in the chalcopyrite field is nonlinear, whereas a linear behavior is observed for the zinc blende alloys. The linear behavior begins at different points on the different lines, and the compositions at which this occurs can be taken as the boundary of the chalcopyrite field. The values for the boundaries estimated in this way are indicated in Fig. 2. However, these estimates are only approximate and, as reported previously (*3*, *4*), a better value of the boundary position is given by the optical energy gap data discussed below.

As is seen from Fig. 3, if the a vs z lines in the single-phase range are extrapolated to $z = 1.0$, they coincide at a value of $a = 0.6333$ nm which represents the value of a that MnTe would have in the zinc blende structure. This is in good agreement with the equivalent value obtained for the $Cd_xZn_yMn_zTe$ alloy (*10*) and also with the value already obtained (*3*, *4*) for alloys of this type.

However in the chalcopyrite field the variation of a with composition is nonlinear. Similar results have been observed in other related alloy systems (*3*, *7*). One possible reason for this behavior is that the de-

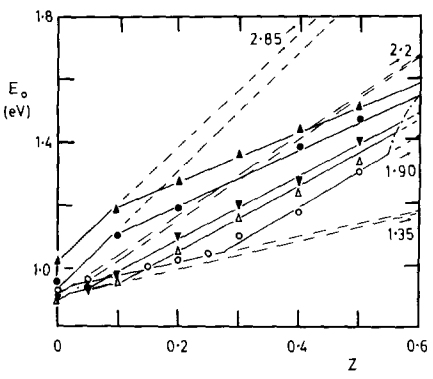

FIG. 5. Variation of room temperature energy gap E_0 with z for various p/y ratios. (○) $p = 0$, (△) $y = 3p$, (▼) $p = y$, (●) $p = 3y$, (▲) $y = 0$. Values shown on dashed lines are the E_0 aiming points in eV at $z = 1.0$.

gree of chalcopyrite order decreases as the amount of either CdTe or MnTe is increased. However, another possible factor is that of nonstoichiometry in samples produced by different growth methods. Thus, systematic changes in the degree of nonstoichiometry with composition could produce a nonlinear variation in lattice parameter values.

As was observed in earlier work on the $Cd_{2w}(CuIn)_yMn_{2z}Te_2$ (*3*) and $Cd_{2w}(AgIn)_xMn_{2z}Te_2$ (*4*) alloys, and more recently reported by Aresti *et al.* (*5*), study of the X-ray photographs showed that for some of the single-phase alloys, faint lines could be observed, indicating the presence of an ordering different from that of the chalcopyrite structure. From magnetic data (*8*), these results have been attributed to ordering of the Mn atoms on the cation sublattice, in both the zinc blende and chalcopyrite structures. However the structures of these ordered phases have not as yet been determined. Recent work on $T(z)$ phase diagrams (*6, 7*) indicates that these ordered phases occur only in the lower temperature range (i.e., $T \leq 400$°C) and so the effects of ordering are most likely to be seen in samples slowly cooled to room temperature or annealed below 400°C.

As indicated above, the variation of the parameter a with z was linear within the limits of experimental error and hence could not be used to show the boundary of this ordered field. Also, because of the very low intensity of the ordering lines, the boundary could not be estimated with any accuracy from intensity measurements either. However, once again as discussed below, the values of the optical energy gap were found to give a good indication of the range in which this ordered structure occurs.

V. Energy Gap Results and Analysis

Optical absorption measurements were made on most of the single-phase samples. It is well known that both CdTe and $CuInTe_2$ are direct band gap semiconductors and previous work (*3, 4*) has shown that the $Cd_{2w}(CuIn)_yMn_{2z}Te_2$ and $Cd_{2w}(AgIn)_xMn_{2z}Te_2$ alloys also have direct gaps. Therefore, plots of $(\alpha h\nu)^2$ vs $h\nu$ were used throughout to determine optical energy gap E_0 values, the higher values of $(\alpha h\nu)^2$ being linearly extrapolated to zero to give a value of E_0. The resulting variation of E_0 with z for various lines of constant p/y ratio is shown in Fig. 5, and as a function of p at constant z in Fig. 6. It has been shown in previous work on alloy systems of this type (*3, 6, 7, 10*) that E_0 varies linearly with z inside any given field and that the aiming point of the E_0 vs z line at $z = 1$ is characteristic of the structure concerned. This parameter takes the following values: for Mn-disordered zinc blende 2.85 eV, for Mn-ordered zinc blende 1.95 eV, and for Mn-ordered chalcopyrite 1.35 eV. For the case of Mn-disordered chalcopyrite, the range of composition available is small and so no accurate determination of the aiming point value has so far been made. The value lies somewhere between 2.2 eV as suggested in the case of $(AgGa)_{1-z}Mn_{2z}Te_2$ (*4*) and $(CuGa)_{1-z}Mn_{2z}Te_2$ (*13*) alloys. In Fig. 5

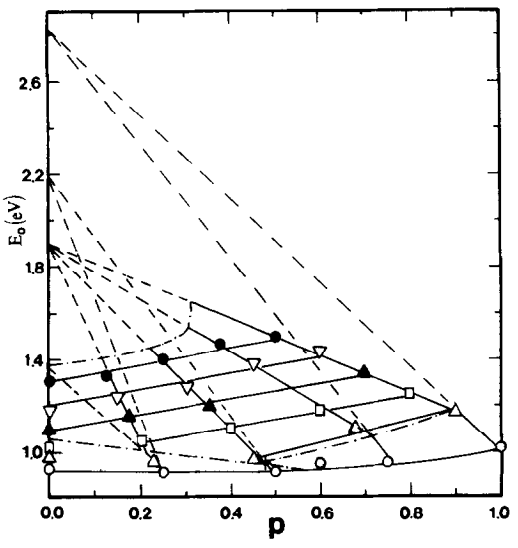

FIG. 6. Variation of room temperature energy gap E_0 with p for various constant values of z. (○) 0.0, (△) 0.1, (□) 0.2, (▲) 0.3, (▽) 0.4, (●) 0.5. ·····, Phase boundaries.

it is seen that the values of E_0 in the Mn-ordered zinc blende and chalcopyrite fields of the present alloys are in good agreement with these previous values. It is to be noted that these alloys will give the E_0 value for the Mn-ordered phase even if the method of preparation is such that some of the high-temperature Mn-disordered phase is still present. This is because the E_0 value of the ordered phase in all cases is lower than that of the disordered phase and so in the optical absorption measurements, the absorption edge of the ordered phase occurs at lower energies and completely masks the edge corresponding to the disordered phase.

These E_0 aiming point values can be used to determine or confirm the position of the boundaries between the various fields. Thus, in Fig. 5, the values of E_0 on the $z = 0$ edge for the $y = 0$ and $p = 3y$ lines have been joined to the value of 2.85 eV at $z = 1.0$ and the points of intersection of these lines with the corresponding ones through the experimental values for $z \sim 0.1$ have been taken as the boundary between the Mn-disordered and Mn-oriented zinc blende fields. In the case of the lines $p = 0$, $y = 3p$, and $p = y$, the values of E_0 on the $z = 0$ edge have been joined to the value of 2.2 eV and again the points of intersection of these lines with the ones through the experimental values for $z \geq 0.05$ have been taken as the boundary between the Mn-disordered and Mn-ordered chalcopyrite fields. (Because of the small composition range of disordered chalcopyrite, even if the working point of 2.85 eV had been used, the estimated position of the boundary would change by a very small amount.) A similar construction has been carried out in Fig. 6 to give the boundary between the Mn-ordered chalcopyrite and the Mn-ordered zinc blende fields. The positions of these boundaries are shown in Fig. 2. These boundary estimates are approximate in that they assume that E_0 is the same on both sides of the boundary, which need not be the case. Inspection of the E_0 graphs indicates that the maximum error to be expected in the estimate of the boundary positions is ± 0.05 in composition.

VI. Conclusions

In a study of semimagnetic semiconductors, both zinc blende and chalcopyrite single-phase fields are of interest and a wide range of single-phase behavior allows better comparison of magnetic properties. It has already been shown (*3*, *4*) that it is possible to substitute Mn onto the $CuInTe_2$ and $AgInTe_2$ lattices providing that equal numbers of *I* and *III* atoms are simultaneously replaced by Mn, and that single-phase solid solution occurs over a large composition range. Furthermore, because of single-phase solid solution over the complete composition range of the $(AgCd_2In)_{1-y}(CuIn)_{2y}Te_4$ line and wide ranges of single-phase solid solution for the $(AgCd_2In)_{1-z}Mn_{4z}Te_4$ and $(CuIn)_{1-z}Mn_{2z}Te_2$ lines, a wide range of single-phase behavior occurs

in the section $(AgCd_2In)_p(CuIn)_{2y}Mn_{4z}Te_4$ ($p + y + z = 1$) and also over an appreciable part of the complete composition diagram (Fig. 2).

Over most of the single-phase region it is found for both zinc blende and chalcopyrite structures that in the lower temperature range the Mn atoms enter preferentially certain cation sites giving some degree of order. The structures of these Mn-ordered lattices, α' and β', have not as yet been established and neutron diffraction work is being carried out to determine these ordered structures. For low values of z, i.e., $0 \leq z \leq 0.1$, the Mn ordering does not occur and so the Mn-disordered phases α and β are observed at lower temperatures. All four of these phases show semiconductor behavior and it is found that the value of the optical energy gap E_0 and its variation with composition depend upon the structure concerned. This result can be used to delineate the boundaries between the four fields.

All of the alloys produced have Mn distributed through the cation sublattice and so show behavior typical of semimagnetic semiconductors. However, the arrangement of the Mn atoms on the cation sublattice is an important factor in determining the magnetic properties, so that the magnetic behavior of the Mn-disordered and the Mn-ordered phases show appreciable differences even for the same Mn concentration. This magnetic behavior is discussed elsewhere (*8*).

Acknowledgments

The authors are grateful to Dr. Valentina Rivera for assistance with the X-ray work, to Mr. F. Sanchez for technical assistance, and to Margarita P. de Quintero for typing the manuscript. They also thank Consejo de Desarrollo Cientifico Humanistico y Tecnologico (DCHT), and CONICIT, Venezuela, for financial support.

References

1. J. A. GAJ, *J. Phys. Soc. Japan* **49,** 797 (1980).
2. J. K. FURDINA, *J. Appl. Phys.* **53,** 7637 (1982).
3. M. QUINTERO, L. DIERKER, AND J. C. WOOLLEY, *J. Solid State Chem.* **63,** 110 (1986).
4. M. QUINTERO AND J. C. WOOLLEY, *Phys. Status Solidi A* **92,** 449 (1985).
5. A. ARESTI, L. GARBATO, A. GEDDO-LEHMANN, AND P. MANCA, "Proceedings of the 7th International Conference on Ternary and Multinary Compounds," p. 497, Materials Research Society (1986).
6. M. QUINTERO, P. GRIMA, R. TOVAR, G. S. PEREZ, AND J. C. WOOLLEY, *Phys. Status Solidi A* **107,** 205 (1988).
7. M. QUINTERO, R. TOVAR, AND J. C. WOOLLEY, *J. Solid State Chem.* **75,** 136 (1988).
8. J. C. WOOLLEY, G. LAMARCHE, A. MANOOGIAN, M. QUINTERO, L. DIERKER, M. AL-NAJJAR, D. PROULX, C. NEAL, AND R. GOUDREAULT, "Proceedings of the 7th International Conference on Ternary and Multinary Compounds," p. 479, Materials Research Society (1986).
9. E. GUERRERO, M. QUINTERO, AND J. C. WOOLLEY, *J. Appl. Phys.* **63,** 2252 (1988).
10. B. BRUN DEL RE, T. DONOFRIO, J. E. AVON, J. MAJID, AND J. C. WOOLLEY, *Nuovo Cimento D* **2,** 1911 (1983).
11. R. G. GOODCHILD, O. H. HUGHES, S. A. LOPEZ-RIVERA, AND J. C. WOOLLEY, *Canad. J. Phys.* **60,** 1096(1982).
12. J. P. SHAY AND G. H. WERNICK, "Ternary Chalcopyrite Semiconductors," pp. 4, 110, Pergamon Press, New York (1975).
13. M. QUINTERO, P. GRIMA, R. TOVAR, R. GOUDREAULT, D. BISSONNETTE, G. LAMARCHE, AND J. WOOLLEY, *J. Solid State Chem.*, in press.